Chemical Engineering Journal 264 (2015) 664–671

Contents lists available at ScienceDirect

Chemical Engineering Journal

journal homepage: www.elsevier.com/locate/cej

A versatile Carberry-type microcatalytic reactor for transient and/or continuous flow operation at atmospheric or medium pressure

Esteban L. Fornero, José L. Giombi, Dante L. Chiavassa, Adrian L. Bonivardi, Miguel A. Baltanás *

INTEC (Instituto de Desarrollo Tecnológico para la Industria Química-UNL/CONICET), Güemes 3450, S3000GLN Santa Fe, Argentina

HIGHLIGHTS

- A novel Carberry-type well-mixed catalytic microreactor is presented.
- Both batch (transient) or continuous operation is feasible.
- Carefully controlled temperature and pressure (up to 3 MPa) conditions achievable.
- Continuous measurement of gas phase composition by mass spectrometry is provided.
- The device performance was validated by comparing measured reaction rates with literature data.

ARTICLE INFO

Article history:
Received 27 August 2014
Received in revised form 13 November 2014
Accepted 23 November 2014
Available online 28 November 2014

Keywords:
Microcatalytic reactor
Carberry-type
Transient experiments
Kinetic regime

ABSTRACT

A novel catalytic reaction device featuring a Carberry-type well-mixed microreactor built inside a medium pressure leak valve is presented. The complete reaction system allows a broad range of kinetic reaction engineering and heterogeneous catalysis studies for both batch (transient) and continuous operation. Carefully controlled temperature (±0.2 K) and pressure (up to 3 MPa) conditions can be achieved. The continuous sampling of the reacting mixture permits instantaneous evaluation of the gas phase composition.

The device performance was validated by comparing methanol synthesis reaction rates for H_2/CO_2 mixtures obtained under transient conditions using this catalytic microreactor with steady-state kinetic rate expressions obtained using a conventional plug-flow microreactor employing the same Pd–GaO*x*/SiO_2 catalyst. Excellent agreement was found.

The reaction was also studied using a more active commercial methanol synthesis catalyst to assess the impact of heat and mass transfer resistances. For the full range of process conditions that was tested, the microreactor operated well under the kinetic regime.

1. Introduction

The use of heterogeneous catalytic reactors for reaction engineering studies and catalyst screening at the laboratory scale is essential. In both cases, kinetic and mechanistic information must be extracted from experiments in which the desired catalytic reaction proceeds together with secondary reactions, physicochemical equilibria, and/or transport processes [1]. A careful choice of operating conditions and complementary studies can eliminate many of these confounding variables, but the type of reactor used and its size and geometry are key factors in minimizing the mass and energy transfer resistance to obtain *intrinsic* chemical kinetic data. In this regard, novel and continued efforts appear, using either particular techniques (e.g., SSITKA [2]) or special designs [3,4] for transient experiments.

Plug-flow (PFR) and continuous flow stirred tank reactors (CSTR) are the traditional tools for kinetic studies under steady-state conditions. Neglecting economic issues (such as those related to isotopic studies), these devices must be operated at low conversion to avoid concentration or temperature gradients at the expense of higher experimental error in the analytical measurements [5]. Discontinuous (batch) reactors, however, are not widely used in heterogeneous catalysis studies due to several drawbacks, although each can be resolved:

- Catalyst deactivation may complicate the analysis. Stabilization of the catalyst prior to the batch experiment and between runs can resolve this issue.
- Batch reactors intrinsically operate in a transient regime, which means that a steady-state composition of chemisorbed reactants and intermediates on the catalyst surface may not be reached. The previous strategy can be employed here, also.

* Corresponding author. Tel.: +54 (342) 455 9175; fax: +54 (342) 455 0944.
E-mail address: tderliq@santafe-conicet.gov.ar (M.A. Baltanás).

http://dx.doi.org/10.1016/j.cej.2014.11.106
1385-8947/

– If only the final composition is measured, only average molar fractions are available for calculations. Periodic extraction or continuous sampling of minute gas amounts can minimize this issue.
– In reactions in which there is a stoichiometric change in the number of moles ($\Delta\nu \neq 0$), such as in the Fischer–Tropsch process, methanol or higher alcohol syntheses, or methanation, there is an intrinsic continuous pressure change. This can be accounted for by using differential conversion data and/or employing internal standards.

Despite these disadvantages, batch reactors allow performing chemical reaction engineering experiments with very low reactant consumption and can additionally be used to extract unique information related to the catalyst response under non steady-state, transient conditions [6–8].

Under these premises, a versatile batch/flow reaction device was built. The core of the unit is a well-mixed ('gradientless') Carberry-type microreactor that suppresses all gradients in the gas phase, thereby maximizing heat and mass transfer between phases [9]. The device is similar to others previously reported in the literature [10,11] but offers some advances in versatility (it can be operated as either a CSTR or a batch reactor) and operating pressure range (it can be evacuated/flushed under moderate vacuum and operated at up to 3 MPa). The reaction device was tested and validated using a demanding reaction system, the selective synthesis of methanol via the hydrogenation of carbon oxide(s), as a model reaction. Many of these reactions must be conducted at moderate to high pressure to overcome thermodynamic constraints and yield a significant conversion.

In the following sections, design details and operating protocols of the microreactor are presented together with data validation employing two different methanol synthesis catalysts, Ga_2O_3–Pd/SiO_2 and CuO/ZnO/Al_2O_3.

2. Experimental

2.1. Microreactor design and features

Two identical small volume cylindrical compartments (~37 cm^3 ea.) made of 316 stainless steel enclosed in a thermostatized oven and interconnected by a high rating (high purity, high pressure-high vacuum, high temperature) bellows valve, constitute the core of the reaction device (Fig. 1). For the batch operating mode, the first compartment acts as a premixer/homogenizer of the reaction mixture. The composition of this mixture can be adjusted at will using a dosing manifold, as detailed below.

Each compartment accommodates a small, removable, magnetically stirred Carberry-type spinning basket [12,13] that can be filled with crushed and sieved particles of the catalyst to be studied and (optionally) with a particulate, inert solid in the premixer. The structure of the spinning device comprises a 316 SS central axle, four baskets made of 250 mesh stainless steel cloth, a horizontal gold-plated mild steel bar on the bottom and a removable cross of top-bladed basket lids. The blades are flat and welded at 45° to ensure good mixing and gas recirculation. The central axle rotates freely by means of two ball bearings. A flexible metal 'spider' made of pure silver gently presses the upper ball bearing against the axle, thus allowing smooth, effortless rotation. All of the removable components, as well as the internal parts of the premixer and the reactor, are gold plated. Magnetic stirring is achieved by means of high temperature Sm2Co17 permanent rotating magnets (T_{max} = 723 K, Electron Energy Corporation, Landisville, PA, USA) driven by variable speed motors.

The premixer and the reactor are constituted by two cylindrical pieces. Both bases are mechanized from stainless steel Conflat type flanges (CF 275). The upper portion of the premixer is an inverted cup, whereas the upper part of the reactor is a bakeable (up to 723 K), high-pressure variable leak valve (AVAC, Redwood City, CA, U.S.A.) that can sustain up to 34 bar with ultra-small gas leaks (1×10^{-8} Torr^{-1} s^{-1}; 3×10^{-13} mol s^{-1} at 523 K). Sealing is achieved by electrolytic copper washers. The bases of both compartments are bolted to aluminum heating blocks inside which heating cartridges are placed. Thermostatic conditions can be precisely set by means of Pt100 thermo-resistances and independent PID temperature controllers. Unless otherwise noted, inlets and outlets are standard welded VCR fittings with metal seals to grant maximum flexibility with regard to pressure or vacuum operation of the units.

As indicated in the Introduction section, the microreactor can operate either in batch or continuous flow modes. The latter is indispensable for catalyst pretreatment, preconditioning or stabilizing/aging procedures. To this end, a soft contact, gold-plated (T-type) piston valve with Kalrez seals, integrated to the reactor compartment base, was designed (Fig. 1).

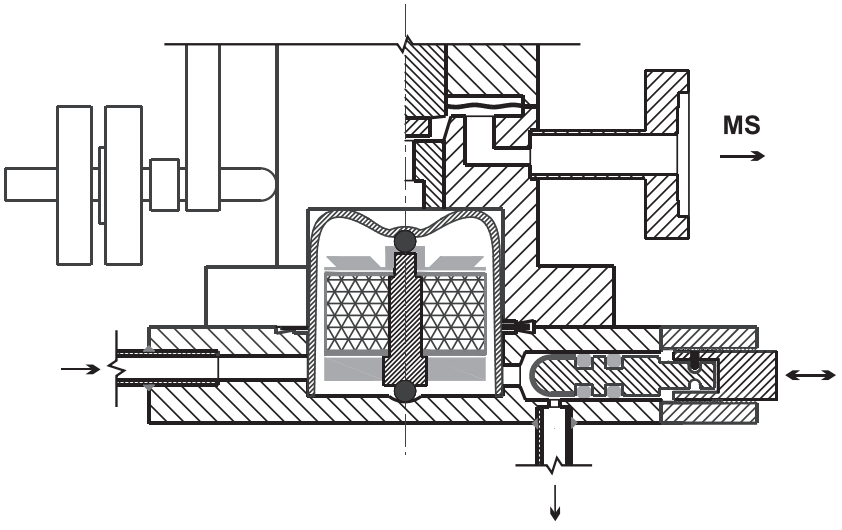

Fig. 1. Scheme of the microreactor and internals (For details, see Supplementary Information).

2.2. Proof-of-concept setup

A minimum-volume, high-purity, evacuable and pressurizable manifold featuring a complete dosing/feeding module was assembled and attached to the microreactor (Fig. 2). The module was specially built for studying methanol synthesis and methanol steam reforming reactions under transient conditions.

Independent lines, each with corresponding line filters, mass-flow controllers and gas purifiers, were provided for inert or reacting gases (Ar, He, H_2, CO, CO_2, H_2/CO_2/He certified mixture, etc.). Water vapor was fed using a dedicated, two-stage microdosing line. Prior to dosing, a small thermostatized vessel half-filled with doubly distilled water was heated and appropriately vented. Condensation was avoided by means of a tracing wire.

The pressure inside the dosing manifold was measured using three 6" dia. precision manometers: a manovacuometer, a low pressure (0–1 MPa) and a medium pressure (0–10 MPa) one. The latter were furnished with isolating metal diaphragms to minimize dead volume and prevent residual contamination. The valves connecting to the manifold were high-purity, heatable bellows type with VCR fittings, allowing either high vacuum (>10^{-6} Torr) or medium pressure (<7 MPa) with a maximum temperature rating of 473 K.

Catalyst pretreatment and preconditioning/aging under steady flow operation under pressure were made possible by means of a back-pressure regulator. Provisions for partial (i.e., manifold section) and or complete evacuation of the internal volume of the reaction system (base pressure ~10^{-5} Torr) were also taken. Lastly, a 64-channel mass spectrometer (Residual gas analyzer Balzers QMS 421, 0–300 atomic mass units range) with a QMH 400-5 quadrupole, secondary electron multiplier (SEM) and Faraday cup detectors was employed to continuously measure the gas composition inside the microreactor (Fig. 2).

Because the premixer and the microreactor have about the same volume, for batch-mode (transient operation) it is straightforward to prepare any reaction mixture in the premixer by doubling the desired pressure. After an initial evacuation of the entire reaction system, successive filling of the evacuated manifold with each reactant up to the required partial pressure followed by its addition to the premixer allowed easy preparation. The final mixture was then transferred to the microreactor by opening the interconnecting, high-rating valve while keeping both baskets rotating at low speed. Pressure equilibration was attained in less than 1 min, after which the interconnecting valve was closed and the basket rotation in the microreactor was set slightly above 700 rpm (the minimum experimental value for which external heat and mass transfer resistances became undetectable, as discussed below). Reproducible compositions of the desired mixtures were achieved (max. error <3% by comparison with certified mixtures).

For continuous operation, a by-pass interconnection between the manifold and the back pressure regulator allowed easy fine tuning of the gas composition with a gas meter prior to any run.

2.3. Validation protocols and measurements

Reaction rate measurements in batch (transient) mode were performed to check the validity and reliability of the kinetic rate data obtained using two well-studied methanol synthesis catalysts. For the validation tests, a gallia-promoted palladium catalyst, Ga_2O_3–Pd/SiO_2 (2 wt.% Pd; 278 $m^2\,g^{-1}$; Ga/Pd = 3 at/at, stabilized [14]) was employed. A more active commercial $Cu/ZnO/Al_2O_3$ catalyst (BASF S3-85; $CuO/ZnO/Al_2O_3$ = 31.7/49.5/18.8 wt.%; 82 $m^2\,g^{-1}$ and 15.5 m^2 Cu g^{-1} after reduction [15]) was used to verify the absence of transport limitations. The composition of the reaction mixture was H_2/CO_2/He = 75/22/3.

The catalysts were pelletized (~0.25-mm-thick, 1-cm-dia. disks) and crushed to make small particles (−20/+30 Tyler mesh size). The palladium-based catalyst was reduced under H_2 flow (50 ml min^{-1}) with a heating rate of 2 K min^{-1} from room temperature to 523 K and then holding for 2 h, after which the premixer and reactor sections were cooled to the reaction temperature, 498 K. The commercial catalyst was reduced following the manufacturer's recommended protocol, using 25%H_2/He flow

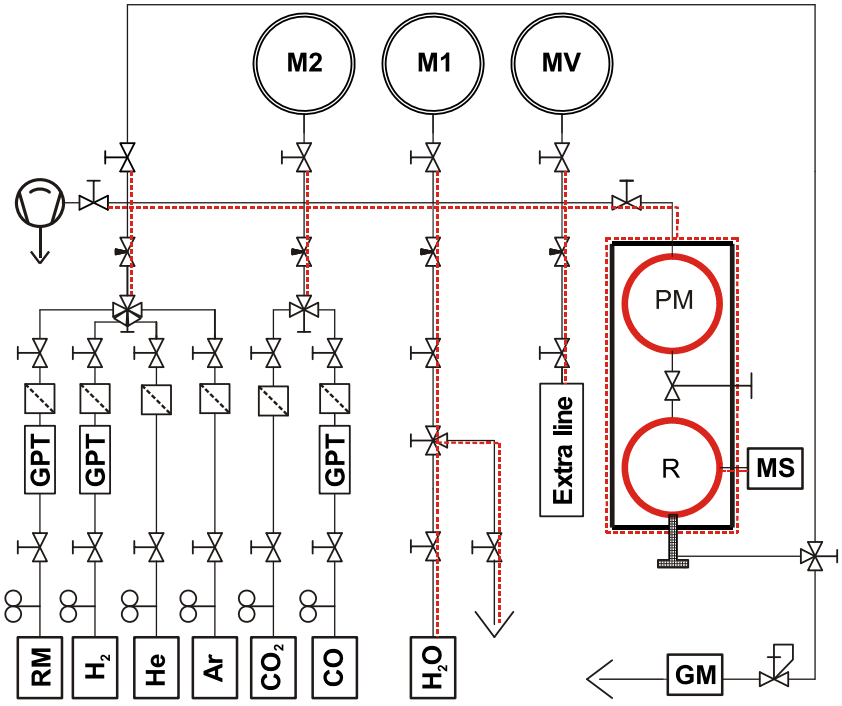

Fig. 2. Proof-of-concept layout: scheme of the complete reaction system: R: microreactor; PM: premixer; MS: mass spectrometer; M1, M2: manometers; MV: manovacuometer; GM: gas meter; RM: reaction mixture; GPT: gas purification train.

(50 ml min^{-1}) with a heating rate of 0.5 K min^{-1} from room temperature to 523 K, also holding for 2 h. The reaction mixture was loaded in the premixer at 3.2 MPa and then introduced in the microreactor, as described above. Blank runs, using the reaction mixture with the empty reactor, ensured the absence of any conversion of the device under these experimental conditions.

The instantaneous composition inside the microreactor was calculated by a double (daily) calibration of the mass spectrometer readings with the $H_2/CO_2/He = 75/22/3$ reaction mixture and the 'thermodynamic equilibrium mixture' under such reaction conditions. Analytical and computational details are given in the appendices.

Ultra high purity gases were used (H_2, He and Ar INDURA, grade 5; H_2/CO_2/He, INDURA certified mixture; CO_2 and CO, 99.99 pure). Silica gel was used to eliminate water traces. CO was purified using crushed quartz (−20/+30 Tyler mesh) at 473 K to decompose carbonyls.

2.4. Microreactor mixing timescale

The timescale of mixing inside the microreactor was assessed by means of a step change in the concentration of a tracer gas fed into the closed vessel. The empty reactor (with the internals but without any particulate solids inside the stirring basket) was filled with helium, and a dose of CO ($y_{CO} = 2.2\%$) was injected through a high temperature silicone septum placed instead of the piston valve at 493 K and 700 rpm.

3. Results and discussion

3.1. Validation of reaction kinetics data

As stated above, transient (batch mode) methanol synthesis experiments were performed employing a standard H_2/CO_2 mixture under realistic process conditions ($H_2/CO_2/He = 75/22/3$ v/v; 1.6 MPa; 498 K) using a stabilized Ga_2O_3–Pd/SiO_2 catalyst. Fig. 3 shows the evolutions with time of the H_2, CO_2, CH_3OH, CH_3OCH_3, CO and H_2O molar fractions inside the microreactor. Because this catalyst produces negligible methanol from CO [16], these results allow an excellent assessment of the stoichiometric balance, as the combined molar fractions of methanol, carbon monoxide and (3 times) dimethyl ether must be approximately equal to the molar fraction of water:

Reaction								$\Delta H^{o}_{298\ K}$ (kJ/mol)	
CO_2	+	$3H_2$	↔	CH_3OH	+	H_2O		−49.58	R_1
CO_2	+	H_2	↔	CO	+	H_2O		41.12	R_2
$2\ CO_2$	+	$6\ H_2$	↔	CH_3OCH_3	+	$3\ H_2O$		−122.66	R_3

It can be readily appreciated from the figure that the stoichiometric balance closure is fairly good (e.g., the molar fractions after 120 min of reaction were: $Y_{H_2} = 72.6\%$, $Y_{CO_2} = 19.9\%$, $Y_{CH_3OH} = 0.4\%$, $Y_{CH_3OCH_3} = 0.1\%$, $Y_{CO} = 1.2\%$, $Y_{H_2O} = 1.8\%$, $Y_{He} = 4\%$). Additionally, the combined molar fractions of CO, CH_3OH and CH_3OCH_3 keep close correspondence with the disappearance of CO_2 (carbon balance closure). Nevertheless, the measured molar fractions of hydrogen and water during the initial period of the reaction (10 min, indicated in dashed lines in the figure) possess an unavoidable, high uncertainty. This is due to the relatively high background pressure of said components inside the sampling chamber of the mass spectrometer before the onset of the transient experiment as a result of the previous pre-reduction of the catalyst with H_2.

Fig. 4 shows the time evolution of the molar fractions of carbon monoxide and methanol (adding twice the amount of dimethyl ether) during the transient experiment, where the confidence interval resulting from the upper and lower bounds taken from

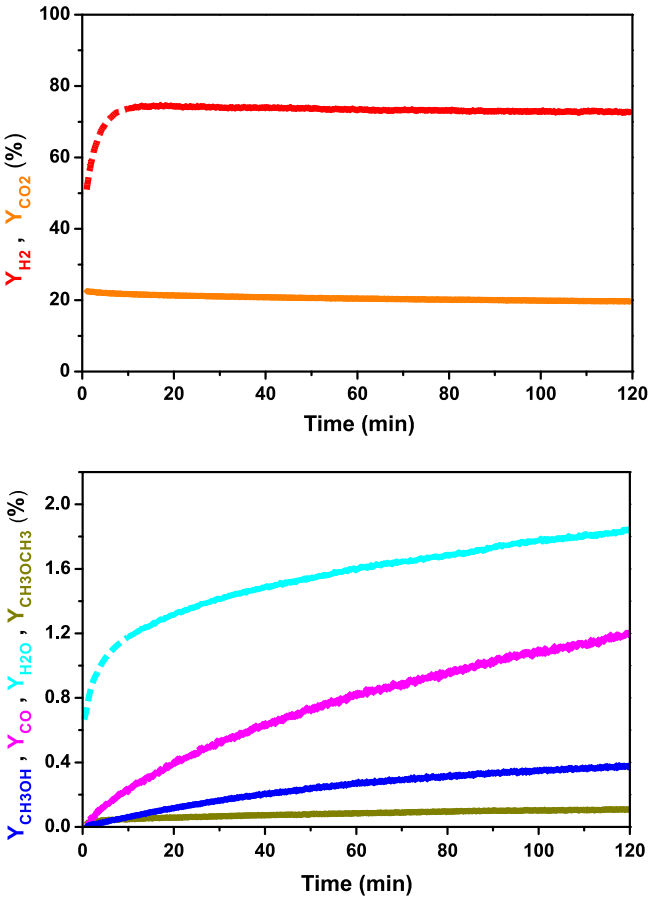

Fig. 3. Time evolution of reactant and product percent molar fractions for the methanol synthesis experiment using the Ga_2O_3–Pd/SiO_2 catalyst (Reaction mixture: $H_2/CO_2/He = 75/22/3$ v/v; 1.6 MPa; 498 K, 460 mg catalyst). Red: H_2. Orange: CO_2: Dark blue: CH_3OH. Magenta: CO. Light blue: H_2O. Dark yellow: CH_3OCH_3, dimethyl ether. The dashed lines in the H_2 and H_2O traces indicate experimental data with high uncertainty (see text). (For interpretation of the references to color in this figure legend, the reader is referred to the web version of this article.)

the calibration values were added to the measured molar fraction of each component. The response of the microreactor to the step change in concentration of CO at 498 K and 700 rpm (i.e., under the same experimental conditions) is included in the figure.

This response follows the simple exponential function $y = 1 - \exp(-t/\tau_M)$, where the characteristic mixing time (τ_M) is 18 s. The CO signal reached its maximum value in approximately 1 min. Conversely, the characteristic time of reactions R_1 and R_2, estimated from the inverse of the derivative of the reaction rate with respect to the degree of advancement of each reaction [$\tau_R = (dR/d\xi)^{-1}$] was more than 30 min, which indicates that the mixing times are negligible with respect to the reaction kinetics. In other words, the characteristic mixing Damköhler number, $Da_{Mix} = \tau_M/\tau_R$, is sufficiently low [17,18].

The transient experiment was then simulated using the kinetic expressions found by Chiavassa et al. for this Ga_2O_3–Pd/SiO_2 catalyst [14]. The kinetic rate equations corresponding to the synthesis of methanol from CO_2 and the reverse water gas shift reaction (RWGS) on this catalyst were obtained by these authors using the Langmuir–Hinshelwood–Hougen–Watson formalism, under the following assumptions: (i) competitive chemisorption of hydrogen and CO on the palladium surface; (ii) competitive chemisorption of atomic hydrogen, carbon dioxide and oxygenated intermediates on the gallia surface and (iii) hydrogenation of the formate intermediate as the *rds*. The authors found the kinetic parameters from steady-state reaction data whereas, in our case,

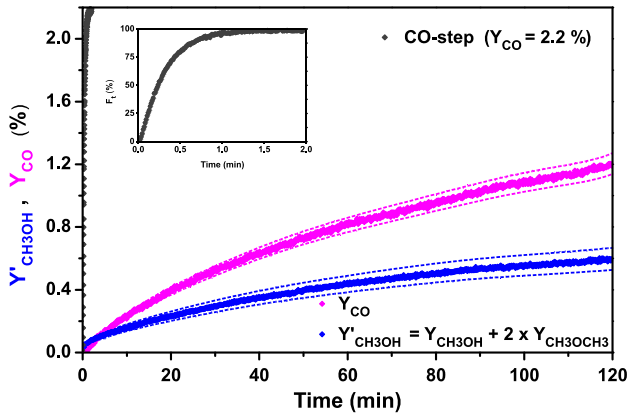

Fig. 4. Comparative time evolution of the percent molar fractions of the reaction products in the methanol synthesis (batch) experiment using the Ga_2O_3–Pd/SiO_2 catalyst (reaction mixture: $H_2/CO_2/He$ = 75/22/3 v/v; 1.6 MPa; 498 K, 460 mg catalyst) versus the time scale of a step change in composition using CO as the tracer gas. Blue: CH_3OH. Magenta: CO-reaction. Gray: CO-step change (repeated in the inset in more detail). Dotted lines: confidence interval of the measured molar fractions, as per the calibration measurements. (For interpretation of the references to color in this figure legend, the reader is referred to the web version of this article.)

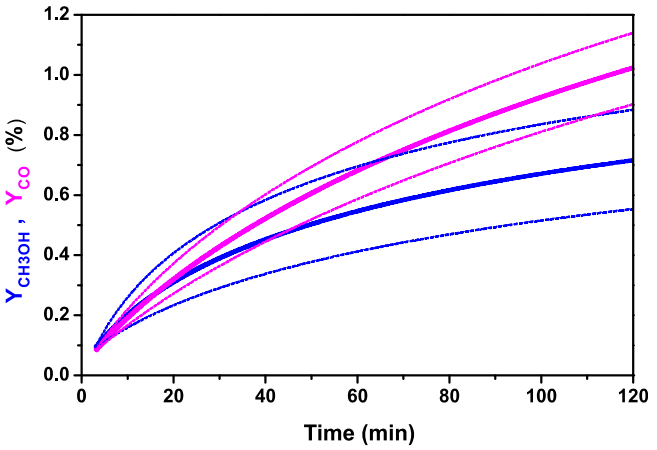

Fig. 5. Time evolution of the percent molar fractions of the reaction products in the methanol synthesis using the Ga_2O_3–Pd/SiO_2 catalyst (reaction mixture: H_2/CO_2/He = 75/22/3 v/v; 1.6 MPa; 498 K, 460 mg catalyst) as per the kinetic model of Chiavassa et al. [14]. Blue: CH_3OH. Magenta: CO. Dotted lines: confidence interval of the calculated molar fractions using the model results. (For interpretation of the references to color in this figure legend, the reader is referred to the web version of this article.)

a transient experiment was performed using the microreactor in the batch mode. This means that upon introducing the reaction mixture (the catalyst was just H_2 pre-reduced), the active sites of the catalyst surface became progressively occupied (filled) with chemisorbed intermediates until a pseudo steady-state was reached. Considering the catalyst's structural and chemical features and the observed initial reaction rates, a maximum transitory ('sites filling') lapse of 1.4 min was estimated (See Appendix C). Consequently, the computational simulation of the experiment used concentration values measured after twice the 'sites filling' time.

The evolution of the calculated (simulated) values of the methanol and carbon monoxide molar fractions is shown in Fig. 5. The upper and lower boundaries of said values using the confidence interval of the model parameters obtained from the non-linear regression routine [14] is also indicated. The experimental and calculated values are in fair agreement (compare Figs. 4 and 5), which gives a strong support to the execution of transient (batch) experiments in this type of microreactor, in lieu of longer and more expensive steady-state runs, whenever a well-characterized catalyst is used. Incidentally, under the studied process conditions, only minor changes occur on the surface of the Ga_2O_3–Pd/SiO_2 catalyst during the 120 min transient experiment after the pseudo steady-state is reached (i.e., after the 'sites filling' period of approximately 1.5 min has elapsed). The effective available exposed metal fraction for hydrogen dissociation, which is affected by the strong CO chemisorption onto Pd, changes from 0.64 down to 0.47 due to the progressively higher CO partial pressure. Nevertheless, the concentration of atomic hydrogen on the gallia surface is approximately 97% of the maximum (chemical equilibrium) value [14].

3.2. Transport limitations

More severe reaction conditions were used to analyze the possible impact of transport limitations in the device by employing a more active commercial Cu/ZnO/Al_2O_3 catalyst under the same experimental conditions ($H_2/CO_2/He$ = 75/22/3 v/v; 1.6 MPa; 498 K). Fig. 6 shows the time evolution of the molar fractions of CH_3OH, CO and H_2O in the microreactor using approximately 1 g of catalyst. The figure includes the calculated values of each molar fraction at thermodynamic equilibrium for a pressure decrease inside the microreactor of *ca.* 0.1 MPa h^{-1} due to the continuous sampling of the gas phase to the MS. It can be promptly appreciated that the reaction products nearly reached their equilibrium values after the 120 min experimental run (approx. error <13%).

The calculated initial reaction rate of methanol synthesis, R_{MeOH}, was 4.7×10^{-7} mol g_{cat}^{-1} s^{-1}. In transient experiments using copper-based catalysts, it is not possible to calculate the initial R_{CO} rate due to the RWGS reaction because the CO_2 reactant also oxidizes the pre-reduced Cu, thus producing an extra quantity of CO [19] that would lead to an overestimation of the reverse water gas shift reaction rate. The characteristic mixing Damköhler number is still sufficiently low here to dispel any concern about the presence of mixing time artifacts.

The absence of external and/or internal heat and mass transfer limitations in heterogeneous catalysts can be checked for both steady-state (in our case, quasi steady-state) and transient conditions. In the first case, the Carberry number (external mass transfer), the Wheeler–Weisz parameter (internal diffusion) and the Prater numbers (for external and internal heat transfer) can be

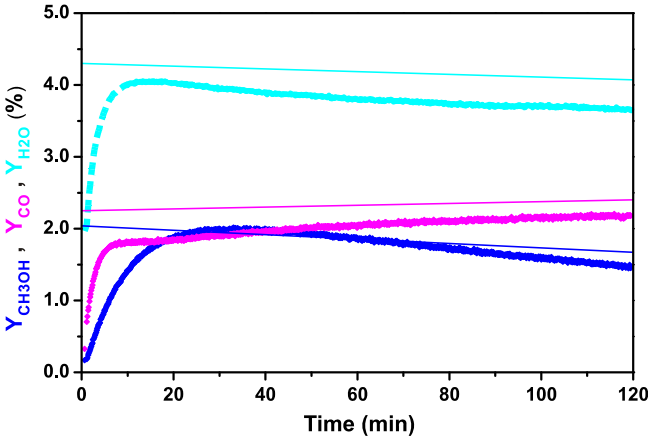

Fig. 6. Time evolution of the percent molar fractions of the reaction products in the methanol synthesis using the commercial Cu/ZnO/Al_2O_3 catalyst (reaction mixture: $H_2/CO_2/He$ = 75/22/3 v/v; 1.6 MPa; 498 K, 1 g catalyst). Blue: CH_3OH. Magenta: CO. Light blue: H_2O. The straight lines indicate the corresponding thermodynamic equilibrium values (see text). (For interpretation of the references to color in this figure legend, the reader is referred to the web version of this article.)

used [20,21], while for truly transient conditions, additional criteria were developed, as indicated in the following sections.

3.2.1. Steady-state operation criteria

Assuming that the (high) initial reaction rate of the methanol synthesis measured with the $Cu/ZnO/Al_2O_3$ catalyst was sustained during steady-state operation, the following results would result (the figures between parentheses correspond to the studied catalyst):

– Absence of external mass transfer limitations, Carberry criterion:

$$\text{Carberry number } (N_{Ca}): \frac{R_{CH_3OH}}{k_g a' C} < 0.01 \quad (1)$$

where R_{CH_3OH} is the volumetric reaction rate (5.66×10^{-7} mol cm^{-3}_{bed} s^{-1}), k_g is the mass transfer coefficient (2.4 cm s^{-1}, taken from data for a similar catalyst [22]), a' is the pellet external area-to-volume ratio (141.5 cm^{-1}) and C is the CO_2 concentration (8.61×10^{-5} mol_{CO2} cm^{-3}). Here, $N_{Ca} = 1.94 \times 10^{-5}$.

–Absence of internal mass transfer limitations, Wheeler–Weisz criterion:

$$\frac{R_{CH_3OH} \cdot L^2}{C \cdot D_e} < 0.1 \text{ [20]} \quad \text{or} \quad \frac{R_{CH_3OH} \cdot L^2}{C \cdot D_e} \cdot \frac{n+1}{2} < 0.1 \text{ [21]} \quad (2)$$

where L is the volume-to-external area ratio of the pellet (7.06×10^{-3} cm), D_e is the effective diffusivity (0.062 cm^2 s^{-1} [22]) and n is the reaction order. For our reaction conditions, the first calculated value is 5.3×10^{-6}. The second criterion can be satisfied for any reaction order assignable to the methanol synthesis reaction: 5.3×10^{-6} $(n + 1)/2 < 0.1$.

– Absence of external heat transfer limitations, Prater number:

$$\frac{|\Delta H| \cdot C}{\rho C_p T (\text{Le})^{2/3}} \cdot N_{Ca} < 0.01 \text{ [20]} \quad \text{or} \quad \frac{k_g \cdot |\Delta H| \cdot C}{h \cdot T} \cdot \frac{E_a}{R \cdot T} \cdot N_{Ca} < 0.05 \text{ [21]} \quad (3)$$

where $|\Delta H|$ is the reaction enthalpy (49,580 J mol^{-1}), is the fluid density (4.42×10^{-3} g cm^{-3}), C_p is the heat capacity of the fluid (11.3.7 J g^{-1} K^{-1}), Le is the Lewis number (3.106, dimensionless), h is the heat transfer coefficient (0.065 J s^{-1} cm^{-2} K^{-1} [22]), E_a is the activation energy (87,500 J mol^{-1} [22]) and R is the gas constant (8.314 J K^{-1} mol^{-1}). For our reaction conditions, the first calculated value is 1.56×10^{-6} and the second one is 1.3×10^{-7}. Both criteria are thereby satisfied.

– Absence of internal heat transfer limitations (Prater number):

$$\frac{|\Delta H| \cdot D \cdot C}{\lambda T} < 0.05 \text{ [20]} \quad \text{or} \quad \frac{|\Delta H| \cdot D \cdot C}{\lambda T} \cdot \frac{E_a}{R \cdot T} \cdot \frac{R_{CH_3OH} \cdot L^2}{C \cdot D_e} \cdot \frac{n+1}{2} < 0.05 \text{ [21]} \quad (4)$$

where λ is the thermal conductivity of the catalyst (0.004 J s^{-1} cm^{-1} K^{-1} [22]). For our reaction conditions, the first calculated value is 0.133 and the second one, 1.5 × 10−5 $(n + 1)/2 < 0.05$, is satisfied for any experimental nth order. It is worth pointing out that the first criterion, which is not satisfied here, was developed for a hypothetical situation under which 100% reactant conversion is achieved inside the pellet (that is, for the maximum concentration, and consequently for the maximum temperature, gradient). In fact, what this strict restriction postulated is that no external heat transfer limitation is to be expected, regardless of the observed reaction rate. For practical purposes, it indicates that beyond a certain level of reactant conversion inside the particles, the observed process will no longer be under the kinetic regime.

3.2.2. Transient operation criteria

Under transient conditions, some reactions proceed faster than they do under steady-state (SS) conditions. To account for these situations, special criteria to guarantee the absence of transport limitations (at least as strict as those for SS) and the gathering of genuine kinetic rate data have been developed. For the $Cu/ZnO/Al_2O_3$ catalyst employed by us, the following results were found:

– Absence of external mass transfer limitations [21]:

$$\tau_{ex} = \frac{k_g \cdot a'}{e_b} \cdot t \geq 2.9 \quad (5)$$

where τ_{ex} is the dimensionless time for extraparticle mass transfer, and e_b is the catalyst bed porosity (0.444, dimensionless). For our reaction conditions, $k_g\ a'/e_b = 764\ s^{-1}$, so that the kinetic regime is well-established after one second.

– Absence of internal mass transfer limitations [21]:

$$\text{For } Bi_m = \frac{k_g \cdot r_p}{D_e} \geq 20 \quad (6)$$

$$\tau_{in} = \frac{D_e}{e_{cat} r_p^2} \cdot t \geq 0.25 \quad (7)$$

where r_p is the catalyst particle radius (0.0125 cm), τ_{in} is the dimensionless time for intraparticle mass transfer, and e_{cat} is the catalyst particle porosity (0.1, dimensionless). For our case, the Biot mass number (B_{im}) is 3000 and $De/e_{cat}\ r_p^2 = 0.64$. Again, the kinetic regime is well-established after one second.

4. Conclusions

The presented gold-plated catalytic reaction device, comprising a premixer and a Carberry-type microreactor, is inert and tight both at medium pressure and under moderate vacuum. It can be operated in either continuous or transient (batch) mode, thus allowing the collection of steady-state or initial reaction rate data, as it features continuous sampling to a mass spectrometer. The complete set up allows catalyst pretreatment *in situ*, as well as the preparation of reactant mixtures, in which the concentration of some components can be just in the parts per million range, with excellent precision (3% maximum error). Magnetic stirring prevents contamination. Perfect mixing is achieved, and external mass and heat transfer limitations can be minimized or eliminated altogether. The small mesh size of the rotating baskets allows the loading of finely divided catalyst particles to minimize internal transport limitations.

The validation studies that were performed using the very demanding (exothermic) methanol synthesis reaction and employing two different synthesis catalysts, Ga_2O_3–Pd/SiO_2 and $CuO/ZnO/Al_2O_3$ (more reactive) confirmed that the microreactor was always operating under the kinetic regime and that the kinetic rate data obtained in the microreactor in the transient (batch) operation mode were fully congruent with former steady-state reaction data (and kinetic rate expressions) gathered from the synthesis catalyst using conventional setups.

Acknowledgments

The financial support of UNL, CONICET (PIP 0278), and ANPCyT (PICT 0836) is gratefully acknowledged by the authors.

Appendix

A. Analytical details

Although the discharge flow of leak valves can be regulated, this discharge flow is directly related to the pressure difference between the microreactor (0.1–2 MPa in our case) and the sampling chamber of the mass spectrometer (0.01 Torr). Whenever the microreactor is operated in the batch mode and, in particular, when the reaction system involves changes in the number of moles, the pressure inside the reactor varies continually, so that changes in the input mass gas flow to the mass spectrometer are unavoidable. The deliberate addition of a small fraction of an inert gas (e.g., He or Ar) as an internal standard overcame this hurdle.

Each gas molecule entering the mass spectrometer exhibits fingerprint fragments in accordance with the selected ionization energy of the cathode. For instance, the $m/z = 31$ signal, which corresponds to the CH_3O^+ cation, is the most important signal from methanol (the other signals have $m/z = 32$, 29, 16, etc.). In experiments related to methanol synthesis, H_2, CO_2, CO, CH_3OH, H_2O, traces of C_2H_6O (dimethyl ether) and CH_4 as well as the internal standard inert gas are simultaneously present. Fig. A.1 illustrates a typical time evolution of mass fragments in a batch run using $H_2/CO_2/He = 75/22/3$. The main signals correspond to $m/z = 2$, 4, 18, 28, 31 and 44 from H_2, He, H_2O, CO, CH_3OH and CO_2, together with low intensity trace signals ($<10^{-9}$ A).

Signal scrambling or interference does occur. The $m/z = 28$ signal, for instance, can originate from either CO or CO_2. This second hurdle can be avoided by using the relative intensity values of the different fragments (m/z signals) of each molecule together with the intensity from their respective, non-interfering fragments (For our proof-of concept case, $m/z = 44$ (CO_2), 40 (Ar), 31 (CH_3OH), 18 (H_2O), 4 (He). For CO_2, for instance, the intensity of the $m/z = 44$ signal can be related to the relative intensity of its $m/z = 45$, 28, 16 and 12 fragments. The intensity of the CO^+ fragment of CO_2 can then be subtracted from the total intensity of the $m/z = 28$ signal to calculate the amount of carbon monoxide in the reacting mixture, and so on for the remaining components of the reacting mixture.

Two daily calibrations were performed to correlate the signal intensities in the mass spectrometer with the respective molar fraction of each component inside the microreactor. The first calibration was made using a blank run, using the same pre-reduction protocol and the same pre-established composition of the reaction mixture but without any catalyst inside the baskets to dismiss any possible 'memory effects' of the device. For the reaction mixture $H_2/CO_2/He = 75/22/3$, for instance, the expected signal intensities of the reactants at $m/z = 2$, 4, 44, etc. were readily obtained. To calibrate the signals of the reaction products, a gas mixture with the thermodynamic equilibrium composition at the same temperature and pressure was used instead. The intensity ratio of each signal with the one from the inert gas was constant after 3 min. from the start of each experiment.

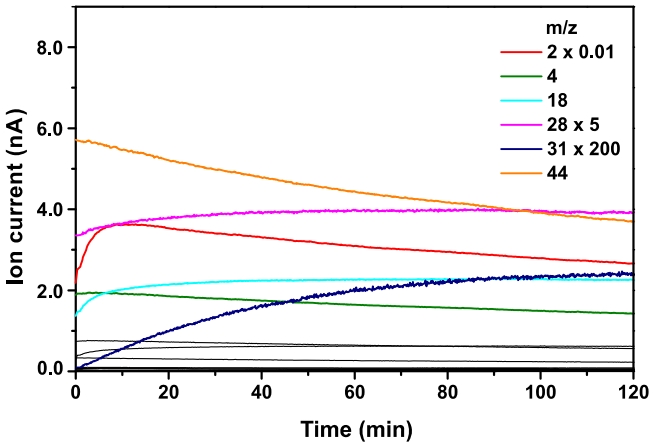

Fig. A.1. Time evolution of the mass spectrometer signals in the methanol synthesis using the Ga_2O_3–Pd/SiO_2 catalyst (batch mode; $H_2/CO_2/He = 75/22/3$ v/v; 1.6 MPa; 498 K, 460 mg cat.). Ionization energy: 90 eV. Main signals: $m/z = 2$, 4, 18, 28, 31, 44. Minor signals: $m/z = 3$, 12, 13, 14, 15, 16, 17, 22, 29, 32, 45, 46 (gray lines).

B. Computational details

The experimental reaction data obtained in the microreactor with the stabilized and pre-reduced Ga_2O_3–Pd/SiO_2 catalyst in batch mode were compared with the kinetic expressions found by Chiavassa et al. for this catalyst under similar reaction conditions using a Berty-type reactor [14].

The mass balance for each reaction component was solved using the Gear routine, namely:

$$d(N_t y_j) = \sum_{i=1}^{2} \upsilon_{ij} \cdot r_i \cdot W \cdot \mathrm{dt} \qquad (8)$$

$$j = H_2,\ CO_2,\ CO,\ CH_3OH \text{ and } H_2O;\ i = 1,\ 2$$

where N_t indicates the total moles inside the reactor, y_j is the molar fraction of the jth component, υ_{ij} is the stoichiometric coefficient of the jth component in the ith reaction, r_i is the specific reaction rate (mol s^{-1} g_{cat}^{-1}), W is the catalyst mass (g_{cat}) and t is the reaction time (s).

C. Ancillary calculations: overall mean surface residence time [7,8] for the Ga_2O_3–Pd/SiO_2 catalyst at 493 K

Data:

- Specific surface (S_{BET}): 278 m^2 g_{cat}^{-1} [16].
- Specific coverage of gallia: 3.35 m^2 g_{cat}^{-1} [23].
- CO_2 adsorption (saturation) capacity of gallia: 2 μmol m_{Ga2O3}^{-2} [24].
- Initial reaction rate at 493 K, 1.6 MPa: 8×10^{-8} mol_{CH3OH} s^{-1} g_{cat}^{-1} (this work).

Specific CO_2 adsorption capacity (Cap):

$$\mathrm{Cap} = 3.35\left[\frac{m^2_{Ga_2O_3}}{g_{cat}}\right] 2\left[\frac{\mu mol_{CO_2}}{m^2_{Ga_2O_3}}\right] \frac{1}{1\times 10^6}\left[\frac{mol_{CO_2}}{\mu mol_{CO_2}}\right]$$

$$= 6.7\times 10^{-6}\left[\frac{mol_{CO_2}}{g_{cat}}\right]$$

Overall mean surface residence time (SRT):

$$\mathrm{SRT} = \frac{\mathrm{Cap}}{R_{CH_3OH}} = \frac{6.7\times 10^{-6}\left[\frac{mol_{CO_2}}{g_{cat}}\right]}{8\times 10^{-8}\left[\frac{mol_{CH_3OH}}{s\cdot g_{cat}}\right]} = 83.7\,[s] \approx 1.4\,[\mathrm{min}]$$

Appendix D. Supplementary data

Supplementary data associated with this article can be found, in the online version, at http://dx.doi.org/10.1016/j.cej.2014.11.106.

References

[1] C. Perego, S. Peratello, Experimental methods in catalytic kinetics, Catal. Today 52 (1999) 133–145.
[2] B.S. Bal'zhinimaev, E.M. Sadovskaya, A.P. Suknev, Transient isotopic kinetics study to investigate reaction mechanisms, Chem. Eng. J. 154 (2009) 2–8.

[3] M.N.A. tSaoir, D.L.A. Fernandes, M. McMaster, K. Kitagawa, C. Hardacre, F. Aiouache, Transient distributions of composition and temperature in a gas–solid packed bed reactor by near-infrared tomography, Chem. Eng. J. 189–190 (2012) 383–392.
[4] J.P. Lopes, S.S.S. Cardoso, A.E. Rodrigues, Interplay between channel and catalyst operating regimes in wall-coated microreactors, Chem. Eng. J. 227 (2013) 42–55.
[5] G. Djéga-Mariadassou, M. Boudart, Classical kinetics of catalytic reactions, J. Catal. 216 (2003) 89–97.
[6] R.J. Berger, F. Kapteijn, J.A. Moulijn, G.B. Marin, J. De Wilde, M. Olea, D. Chen, A. Holmen, L. Lietti, E. Tronconi, Y. Schuurman, Dynamic methods for catalytic kinetics, Appl. Catal. A Gen. 342 (2008) 3–28.
[7] J. Happel, Isotopic Assessment of Heterogeneous Catalysis, Academic Press, New York, 1986.
[8] J.S.J. Hargreaves, S.D. Jackson, G. Webb, Isotopes in Heterogeneous Catalysis, Imperial College Press, London, 2006.
[9] E.C. Meyers, K.K. Robinson, Multiphase kinetic studies with a spinning basket reactor, Proc. 5th Int. Symp. Chem. React. Eng., Houston, EEUU (1978) 447–458.
[10] G. Liu, D. Willcox, M. Garland, H.H. Kung, The rate of methanol production on a copper-zinc oxide catalyst: the dependence on the feed composition, J. Catal. 90 (1984) 139–146.
[11] J.J. Carberry, Designing laboratory catalytic reactors, Ind. Eng. Chem. 56 (11) (1964) 39–46.
[12] D.C. Tajbl, J.B. Simons, J.J. Carberry, Heterogeneous catalysis in a continuous stirred tank reactor, Ind. Eng. Chem. Fundam. 5 (1966) 171–175.
[13] B. Gillespie, J.J. Carberry, Influence of mixing on isothermal reactor yield and adiabatic reactor conversion, Ind. Eng. Chem. Fundam. 5 (1966) 164–171.
[14] D.L. Chiavassa, S.E. Collins, A.L. Bonivardi, M.A. Baltanás, Methanol synthesis from CO_2/H_2 using Ga_2O_3–Pd/silica catalysts: kinetic modeling, Chem. Eng. J. 150 (2009) 204–212.
[15] C.J. Jiang, D.L. Trimm, M.S. Wainwright, N.W. Cant, Kinetic mechanism for the reaction between methanol and water over a Cu–ZnO–Al_2O_3 catalyst, Appl. Catal. A Gen. 97 (1993) 145–158.
[16] D.L. Chiavassa, J. Barrandeguy, A.L. Bonivardi, M.A. Baltanás, Methanol synthesis from CO_2/H_2 using Ga_2O_3–Pd/silica catalysts: impact of reaction products, Catal. Today 133–135 (2008) 780–786.
[17] S.I.A. Shah, L.W. Kostiuk, S.M. Kresta, The effects of mixing, reaction rates, and stoichiometry on yield for mixing sensitive reactions—Part I: model development, Int. J. Chem. Eng. (2012), http://dx.doi.org/10.1155/2012/750162 (article ID 750162).
[18] J. Haber, B. Jiang, T. Maeder, N. Borhani, J. Thome, A. Renken, L. Kiwi-Minsker, Intensification of highly exothermic fast reaction by multi-injection microstructured reactor, Chem. Eng. Proces.: Proc. Intens. 84 (2014) 14–23.
[19] M.S. Spencer, On the activation energies of the forward and reverse water-gas shift reaction, Catal. Lett. 32 (1995) 9–13.
[20] J.J. Carberry, Physico-chemical aspects of mass and heat transfer in heterogeneous catalysis, in: J.R. Anderson, M. Boudart (Eds.), Catalysis, vol. 8, Springer-Verlag, Berlin, 1987, pp. 131–171 (Chapter 3).
[21] F.H.M. Dekker, A. Bliek, F. Kapteijn, J.A. Moulijn, Analysis of mass and heat transfer in transient experiments over heterogeneous catalysts, Chem. Eng. Sci. 50 (22) (1995) 3573–3580.
[22] G.H. Graaf, H. Scholtens, E.J. Stamhuis, A.A.C.M. Beenackers, Intra-particle diffusion limitations in low-pressure methanol synthesis, Chem. Eng. Sci. 45 (1990) 773–783.
[23] S.E. Collins, D.L. Chiavassa, A.L. Bonivardi, M.A. Baltanás, Hydrogen spillover in Ga_2O_3–Pd/SiO_2 catalysts for methanol synthesis from CO_2/H_2, Catal. Lett. 103 (1–2) (2005) 83–88.
[24] S.E. Collins, M.A. Baltanás, A.L. Bonivardi, Infrared spectroscopic study of the carbon dioxide adsorption on the surface of Ga_2O_3 polymorphs, J. Phys. Chem. B 110 (2006) 5498–5507.